



HAL
open science

[Invited] Challenges to measure RF noise and intermodulation performances of mmW/THz devices

Francois Danneville, Haitham Ghanem, Joao Carlos Azevedo Gonçalves, Sylvie Lepilliet, Daniel Gloria, Guillaume Ducournau

► To cite this version:

Francois Danneville, Haitham Ghanem, Joao Carlos Azevedo Gonçalves, Sylvie Lepilliet, Daniel Gloria, et al.. [Invited] Challenges to measure RF noise and intermodulation performances of mmW/THz devices. IEEE Latin American Electron Devices Conference (LAEDC 2022), Jul 2022, Cancun, Mexico. 10.1109/LAEDC54796.2022.9908208 . hal-03791755

HAL Id: hal-03791755

<https://hal.science/hal-03791755v1>

Submitted on 29 Sep 2022

HAL is a multi-disciplinary open access archive for the deposit and dissemination of scientific research documents, whether they are published or not. The documents may come from teaching and research institutions in France or abroad, or from public or private research centers.

L'archive ouverte pluridisciplinaire **HAL**, est destinée au dépôt et à la diffusion de documents scientifiques de niveau recherche, publiés ou non, émanant des établissements d'enseignement et de recherche français ou étrangers, des laboratoires publics ou privés.

Challenges to measure RF noise and intermodulation performances of mmW/THz devices

François Danneville¹, Haitham Ghanem¹, Joao Carlos Azevedo Gonçalves², Sylvie Lepilliez¹, Daniel Gloria², Guillaume Ducournau¹

¹ Univ. Lille, CNRS, Centrale Lille, Junia, Univ. Polytechnique Hauts-de-France, UMR8520 - IEMN - Institut d'Electronique de Microélectronique et de Nanotechnologie, F-59000 Lille, France

² STMicroelectronics, 38926 Crolles, France

Abstract— Applications in millimetre wave range and terahertz frequencies keep on increasing. In this context, drastic challenges are faced at measurement level, in particular to extract noise performance and nonlinear properties of devices and circuits used to build the required systems. The aim of this talk is to provide an overview of these challenges, and to describe the solutions that we have developed to respond to them.

Keywords— mmW, THz, measurement, noise, third order intermodulation point

I. INTRODUCTION

With the continuous growing of communication systems, a major part connected to the internet, an increase of transmission channels capacities is required, and accordingly, the design of communications systems with high data rates [1].

Device technology has greatly evolved for several decades, offering opportunities to increase systems bandwidth. It requires electronics to operate in mmW/THz (that is, frequency higher than 100 GHz) frequency range. In this context, millimeter-wave radars and passive sensors are emblematic solid-state implementations that promise improved performance.

In order to build up a full mmW system, components integration [3,4] is of utmost importance while being highly challenging; in particular, it requires a deep understanding of the various bricks being parts of the system. To do so, a powerful way lies in the characterization of the electronic devices and circuits, carried out through scattering parameters, power, linearity and RF noise measurements.

The aim of this paper is to address measurements challenges identified in mmW/THz frequency range, with special emphasis on RF noise and linearity performance extraction. We will describe first the test bench dedicated to noise measurements up to 325 GHz. It will be followed by a state of the art of available devices such noise sources. Then will follow the modeling/analysis of a broadband integrated diode noise source up to 325 GHz, before using this noise source and an assembled noise receiver enabling noise measurements of active devices up to 260 GHz. Finally, a photonic device UTC-PD is used as a two tone generator to extract the intermodulation points of active devices around 300 GHz.

II. NOISE MEASUREMENTS TEST BENCH

A classical test bench used to measure the noise performance (most often the noise figure) on wafer, is shown in Fig. 1.

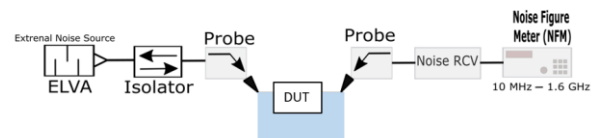


Fig. 1. Bench setup dedicated to noise measurements

As illustrated, an external solid-state calibrated noise source is used, which provides an excess noise ratio (ENR) usually higher than 10 dB. GSG probes are used to connect external instruments to the access pads of the device under test (DUT). Depending on the frequency range of interest, one has to identify an available external noise source as well as to build up the noise receiver (RCV). Finally, a noise figure meter (operating in low frequency range) is performing noise power measurements.

RCV noise figure (NF) is critical and in order to address mmW noise measurements, the frequency range was split in 3 bands: 130-170 GHz, 170-260 GHz and 260-325 GHz. Measured RCV noise figure are provided in Fig. 2.

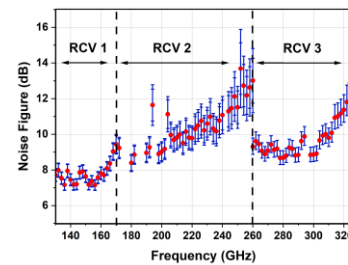


Fig. 2. Extracted noise figure for all receiver structures available

Between 170 GHz and 325 GHz, RCV NF stands between 8.5 dB and 13 dB, required values to perform accurate noise performance in mmW range.

III. INTEGRATED SOLID STATE NOISE SOURCE - AMPLIFIER NF MEASUREMENT IN MMW RANGE

As mentioned in section II, commercial calibrated solid-state noise sources are required to carry out noise measurements in mmW range. They are characterized by their ENR, which sets the noise power level above the thermal noise floor (defined at $T_0 = 290\text{K}$, the “standard” noise temperature). The challenge lies in the availability of such (external) commercial noise sources for frequencies higher than 220 GHz. In this context, silicon technology (that is, BiCMOS 55nm from STMicroelectronics) offers an opportunity for the development of an “integrated” solid-state noise source [5,6].

A. Process description of the solid-state noise source

The intended noise source to be integrated was developed using BiCMOS 55nm technology from STMicroelectronics. It is made using a Schottky like diode, details may be found in [5,6]. For the noise structure, the Schottky diode on the anode is shunted to ground and its cathode connected to a RF-pad (1 port configuration), as shown in Fig. 3. To be used as a noise source, the diode is biased in avalanche regime.

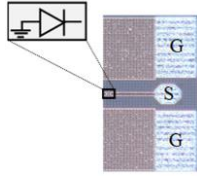


Fig. 3. Diode noise source (1 Port) layout

B. ENR extraction of solid-state noise source

In order to extract the ENR value of the noise source, the setup shown in Fig. 4 was mounted.

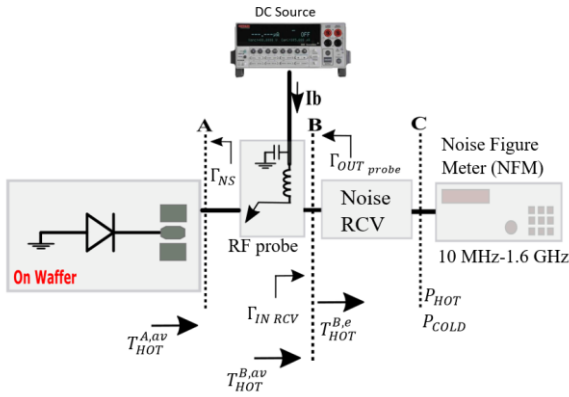


Fig. 4. Setup for ENR extraction of the integrated diode noise source

This setup allows to extract the ENR, defined as follows:

$$ENR_{A,av} = \frac{T_{HOT}^{A,av} - T_{COLD}}{T_0} \quad (1)$$

In (1), T_{COLD} is the noise source temperature when the diode is in the OFF state (equal to the physical ambient temperature, taken equal to T_0), while $T_{HOT}^{A,av}$ is the available hot noise temperature of the noise source when it is turned in

its ON state, extracted using the setup shown in Fig. 4 (details regarding the calculation carried out to extract $T_{HOT}^{A,av}$ can be found in [5]). The noise source achieved an ENR value up to 20 dB in the frequency range 130-260 GHz, as shown in Fig. 5.

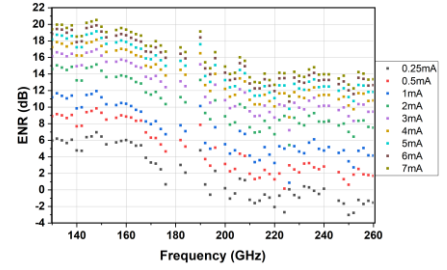


Fig. 5 : Extracted ENR of the integrated noise source up to 260 GHz.

It is to be noted that ENR value decreases with decreasing current, thus, biasing the noise source at low DC current values will lead to insufficient values at the output power of the two-port device under test, thus not detectable by the noise RCV.

C. Noise source electrical model

The theoretical behavior of the solid state noise source was intensively studied [6], a broadband small signal equivalent circuit of the diode (Fig. 6) was extracted and validated between DC to 320 GHz (different S measurement setups were used).

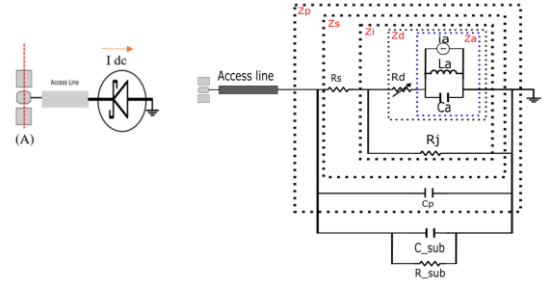


Fig. 6: Broadband small signal equivalent circuit extracted for the schottky diode.

Adding the noise source “ia” (Fig. 6), and knowing its avalanche current spectral density [7], it was possible to simulate the ENR, and to perform a comparison with experimental values, as illustrated in Fig. 7.

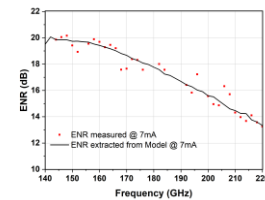


Fig. 7: Simulated and measured ENR curve of the diode of size $3.44\mu\text{m}^2$ biased at 7mA.

A good agreement was observed between expected ENR and the measured one.

D. Importance of ENR: Relation with NF

The ENR is directly linked to the noise figure. For this purpose, let's consider the following circuit (Fig. 8) :

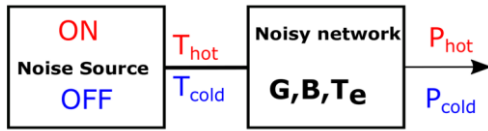


Fig. 8. Noise powers measured at the output of a two-port device, for two noise temperatures of the noise source (corresponding to the ON and OFF states)

If ENR is precisely known, the noise figure NF of the noisy network is straightforward determined by the following formulae [8]:

$$NF = \frac{ENR}{(Y-1)} \quad (2)$$

In (2), Y corresponds to the ratio between the hot and cold output noise powers ($Y = \frac{P_{hot}}{P_{cold}}$) measured at the output of the two-port device (Fig. 8). The cold (hot) output noise power refers to the measured output noise power when the solid state noise source is in its OFF (ON) state.

E. NF Extraction of packaged amplifier in 220 to 260 GHz frequency range

The integrated noise source based on a Schottky diode structure was used to extract the noise figure of a packaged amplifier in 220 to 260 GHz. The set-up used to perform the measurement is shown on Fig. 9.

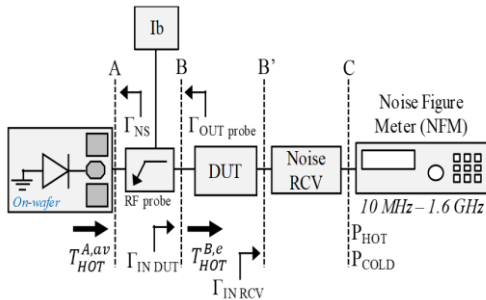


Fig. 9: Block diagram set-up to perform noise characterization of a packaged amplifier up to 260 GHz

For waveguide noise characterization, the amplifier is placed between the RF probe waveguide flange and the input of the noise RCV. Based on the block diagram set-up presented in Fig. 9, the noise source has been used in waveguide flange at plan B, through the RF probe. The diode is contacted by the RF probe and reverse-biased through the bias tee of the RF probe in its avalanche regime. The assembled experiment is presented in Fig. 10.

The amplifier stand alone has a poor matching, so the amplifier is connected with variable attenuators at the input and output planes, to improve the matching to the other stages, even if that will increase the total noise figure of the device (Fig. 10) [5].

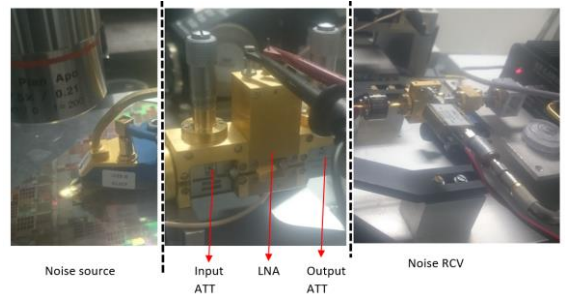


Fig. 10: Test bench set-up to perform noise characterization of a packaged amplifier up to 260 GHz

The measurements and extractions were performed for variable bias current conditions of the diode noise source, between 0.25 mA and 7 mA, as shown in Fig. 11. For biasing currents below 2 mA the extracted noise figure shifts from the extracted values done between 2 mA and 7 mA, this is due to the insufficient noise power supplied by the noise source to the amplifier. This can be seen in Fig. 5 where the ENR value for low biasing currents is very small in this frequency range, and it is further attenuated after the probe.

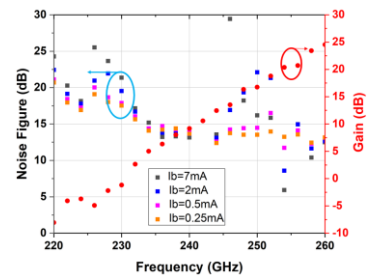


Fig. 11: Extracted noise figure of packaged amplifier using assembled test bench

IV. INTERMODULATION (IP3/IP5) EXTRACTION USING A SINGLE THz PHOTONICS SOURCE

In this part, it is presented how a single THz photonic source can be used to extract the third and fifth intermodulation behavior @300 GHz for a HEMT technology-based low noise amplifier [9].

A. THz Photonics Source for Two-Tone THz Generation

THz photomixing is a versatile technique to generate THz continuous wave (CW) using fast photodiodes. In order to generate a THz signal, two laser sources are required, as shown in Fig. 12.

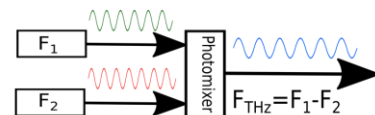


Fig. 12: Schematic illustrating how, using two optical signals, a THz signal can be generated using a photomixer

Nevertheless, if one wants to extract intermodulation products of a solid-state transistor/LNA, it requires two signals (at 299 GHz and 301 GHz, respectively) to be injected

at the DUT input. Hence, three laser sources will be required. The optical signals generated by these lasers are applied to the THz photomixer, that is, a untravelling carrier photodiode (UTC-PD) from NTT Electronics, which generates (if lasers source frequency are carefully chosen) the two-tone THz signals (Fig. 13).

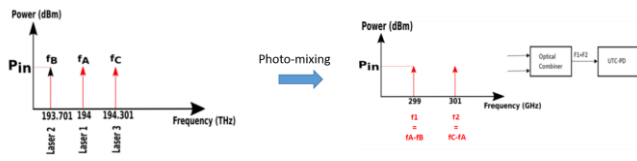


Fig. 13: Two-tone signal generation at 300 GHz using multitone optical signals at $1.55 \mu\text{m}$.

B. Intermodulation Measurement of a LNA

Details regarding the investigated LNA can be found in [9]. The whole set-up used to perform intermodulation products measurement is shown in Fig. 14.

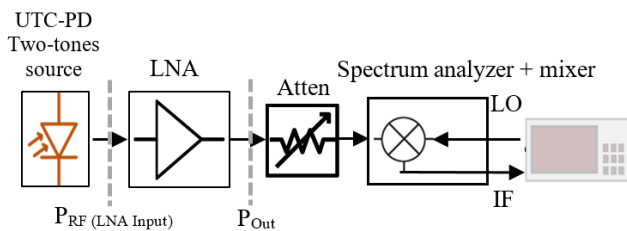


Fig. 14: Measurement of intermodulation of the LNA. Atten is a WR3.4 attenuator used to avoid any saturation of the measurement equipment. The UTC-PD source is here driven with three optical signals to get two CW tones at 300 GHz at LNA input. Accuracy is 0.5 dB for power measurement

The LNA is placed between the UTC-PD and the input of the receiver. The incident power at the LNA input (P_{RF}) is varied by changing the optical power applied to the UTC-PD. At the LNA output, a mixer is used to measure the power of the tones. Increasing the power at the input (frequencies f_1 and f_2 , see Fig. 13), two other tones appear at the LNA output, that are, $(2.f_1 - f_2)$ and $(2.f_2 - f_1)$: the power related to these signals at these two frequencies represent the IP3 signals of the LNA. Measurements results are shown in Fig. 15.

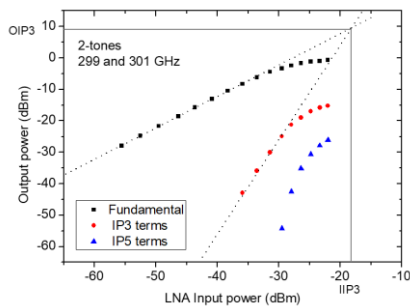


Fig. 15: Measurement of the intermodulation of the LNA using the linear and spurious-free two-tone photonics-based source

From Fig. 15, IP3 is clearly detected, with a slope 1:3, as expected by the theory. The IIP3 intercept point is -18 dBm. As observed in Fig. 15, the setup is also able to extract IIP5, for IP5 is also detected.

C. LNA NF extraction

Though not recalled in this paper, it is to be highlighted that using the same “single” THz photonics source, the noise figure extraction of the LNA (for which IIP3 was extracted in section IV.C), was carried out [9].

V. CONCLUSION

In this paper, challenges encountered for noise and intermodulation measurements in mmW/THz range have been addressed. Special emphasis was made to highlight - in these frequency ranges -, the requirement of high performing noise receiver and integrated noise source to extract device noise performance. Finally, an innovative test bench, marrying optical and solid-state THz concepts, was presented to perform intermodulation measurements.

REFERENCES

- [1] A. Mahdy and J.S. Deogun, “Wireless optical communications: a survey”, IEEE Wireless Communications and Networking Conference, 2004
- [2] I. Sourikopoulos, S. Hedayat, C. Loyez, F. Danneville, V. Hoel, E. Mercier and A. Cappy A., “A 4-fJ/spike artificial neuron in 65 nm CMOS technology”, *Frontiers in Neuroscience*, Volume 11, Article 123, March 2017
- [3] E. Gates and L. Chartrand. Introduction to Electronics. Cengage Learning, 2006
- [4] Bharat Bhushan. Springer Handbook of Nanotechnology. Berlin, Heidelberg: Springer, 2007
- [5] J.C. Azevedo Goncalves et al, “Millimeter-Wave Noise Source Development on SiGe BiCMOS 55-nm Technology for Applications up to 260 GHz”, IEEE Transactions on Microwave Theory and Techniques, Vol. 67, n. 9, 2019
- [6] H. Ghanem et al, “Modeling and Analysis of a Broadband Schottky Diode Noise Source Up To 325 GHz Based on 55-nm SiGe BiCMOS Technology”, IEEE Transactions on Microwave Theory and Techniques, Vol. 68, n. 6, 2020
- [7] M. C. Maya, A. Lázaro, and L. Pradell, “Extraction of an avalanchediode noise model for its application as an on-wafer noise source,” *Microw. Opt. Technol. Lett.*, vol. 38, no. 2, pp. 89–92, Jul. 2003
- [8] “Fundamentals of RF and Microwave Noise Figure Measurements”, application note 57-1, Agilent Technologies, Inc. 2010 Printed in USA, August 5, 2010, 5952-8255E
- [9] H. Ghanem et al, “300-GHz Intermodulation/Noise Characterization Enabled by a Single THz Photonics Source”, IEEE Microwave and Wireless Components Letters, Vol. 30, n. 10, 2020